Estimation of Base Drag for a Subsonic Missile Configuration using CFD

Aman Prakash[1], K. A. Suraj[2] & Ansab Peter[3]
[1]CFD Engineer, DRDL, DRDO, India
[2]Customer Success Engineer, Autogrid India Pvt. Ltd., India
[3]BDM, KYK India Corp Pvt, Ltd., India
***DOI**: https://doi.org/10.34293/acsjse.v4i1.108*

Received Date: 11.01.2024 **Accepted Date:** 28.02.2024 **Published Date:** 01.04.2024

Abstract - *The purpose of the investigation was to comprehend base drag around a subsonic missile in the jet off situation. To quantify the base drag for various base geometries at various velocities and angles of attack, a CFD simulation has been run. When CFD simulation results are compared to those from other CFD solvers, they exhibit good agreement with respect to flow and base drag under cruising conditions.*
***Keywords**: CFD, Subsonic Missile, ANSYS, Base Drag, Pressure*

I INTRODUCTION

The geometry of a body's cross section greatly influences the vortex shape, the reattachment point, and flow separation, especially in the subsonic and transonic regimes. As the edges round off, the flow separation transitions from turbulent to laminar with an angle of incidence. The current study describes a computational analytic method for estimating the aerodynamic properties of three geometrical configurations with circular cross sections: a flight body with a nozzle at the base, a boat tail configuration, and a hemispherical body with a flat base. Figure 1, 2 and 3 represents the flat base geometery, boat tail geometry and nozzle base geometery respectively.

One of the most important aerodynamic performance parameters for flying machines is total drag. The overall drag for flying objects is composed of three components: base drag (iii), viscous drag (skin friction), and pressure drag (i) (not including the base). A major component of the total drag is the base drag. A form of aerodynamic drag known as "base drag" is caused by a partial vacuum in the flight vehicle's tail. The vacuum is the space created when the car passes through the atmosphere. Base drag fluctuates while you fly. This gap is filled by the massive amount of gas the motor produces, which lowers drag while it is operating. At burnout, when this gas runs gone, the drag increases significantly. Base drag reduction and measurement are done. Base drag depends on various geometrical and flow properties. When there is a turbulent boundary layer upstream of the base and no jet flow, the primaryFree-streaming mach number immediately in front of the base

a. The thickness of the boundary layer momentum upstream of the base
b. Base diameter
c. Angle of attack
d. Following body shape (after-body length, after-body diameter, boat-tail or flair angle) and

e. Characteristics of the fundamental drag reduction mechanism

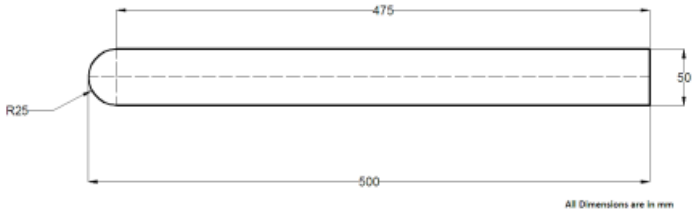

Figure 1 Flat base Geometry

Boat tail drag is the term used to describe the drag generated by the conical part of a ballistic body that gradually reduces in diameter towards the tail in order to reduce overall aerodynamic drag. When comparing the drag of the nozzle shroud arrangement to the base drag, the boat tail has the least amount of drag.

Figure 2 Boat Tail Geometry

An outer shroud encircles the center body of a nozzle shroud, at least in part. An inner side section, an outer side portion, and a forward end portion that is axially separated from an aft end portion are all defined by the main body that is easily spread apart from the outer shroud to provide a pre-mixed flow route.

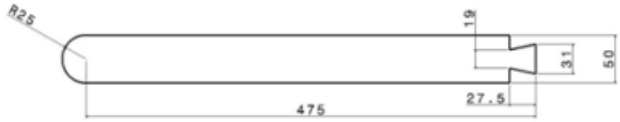

Figure 3 Nozzle base Geometry

II CITATIONS AND LITERATURE REVIEW

Analytical techniques were used to calculate the aerodynamic properties of various components, such as the body, wing, and tail of an anti-aircraft missile, in P. Sethunathan's article on the aerodynamic configuration design of missiles [1]. Using linear wing theory, Newtonian impact theory, and narrow wing theory, the normal force coefficient values were anticipated during the drag characterisation, which was carried out at different Mach numbers at subsonic speeds. The normal force coefficients at various angles of attack (AOA) were also calculated.

The effect of different boat tail designs on base pressure was investigated by Karpov [2]. According to the study, boat tails longer than 0.5 calibers regularly result in a decrease in overall drag. Conical boat tails showed less drag than ogival or concave shapes for boat tail lengths between 0.5 and 1.5 calibers. It was found that the base pressure increased with boat tail angle at the base but decreased with boat tail length.

Wee predicted a missile configuration's static aerodynamic properties using the CFD code ANSYS-CFX [3]. This research examined several Mach values and contrasted the findings with experimental data collected from wind tunnel experiments.

At the Agency for Defense Development (ADD), Kwang Seop Lee and Seungkyu Hong gave examples of CFD validations and uses in aerodynamic design and analysis for missiles [4]. Examples covered included side jet and boat tail interactions in the supersonic flow zone, and several approaches to validate complicated flows were explained.

In an AGARD study [5], George G. Brebner talked about the general aerodynamics of missiles. The research emphasized the disparities in missile geometric dimensions and design goals, which call for various aerodynamic computation techniques. It explored the significance and characteristics of each of the six aerodynamic force and moment components operating on a missile.

To find out how boat tail shape affects the base pressure coefficient, Mitchell et al. investigated a thin body with a square cross-section in a low-speed wind tunnel [6]. Numerical modeling was used in conjunction with the experimental investigation to investigate the after body form for least base drag, covering an angle-of-attack range of 0 to 8 degrees.

Combining theoretical and actual data, Hitchcock et al. described a technique for predicting the head, base, and friction drag coefficient of missiles [7]. The drag coefficient was examined in relation to a typical projectile, taking into account the form factor and Mach number.

In a research by (Frank G), an enhanced empirical model for forecasting base drag on missile configurations was created using fresh wind tunnel data [8]. Angles of attack, fin control deflections, fin thickness to chord ratio, and fin positions were among the variables taken into account by the model.

In their study of controlled base flow separation and drag reduction, (V. Menezes et al.) focused on wake flow challenges at high speeds and how they affect drag in projectile and missile design [9]. The idea of a conical or boat-tailed afterbody was emphasized as a useful way to lower base drag.

III METHODOLOGY

The streamlines would produce a symmetric pattern for low-speed subsonic flow over a sphere or an infinite cylinder with its axis normal to the flow if the flow were inviscid (frictionless). The pressure distributions over the front and rear surfaces would therefore likewise be symmetric. This symmetry leads to an important phenomenon: in the case of a frictionless flow, the sphere experiences no pressure drag. The actual flow over a sphere or cylinder produces split flows at locations where there is a negative pressure gradient when friction is present. There will be high pressure drag, a relatively fat wake, and split flow on the back face of the cylinder; Figure 4 illustrates this situation. The cylinder's total drag is shown by the bar to the right of the picture; skin friction drag is represented by the shaded section of the bar, and pressure drag is represented by the open portion. When dealing with a blunt body, pressure drag accounts for the majority of the drag, which is rather high.

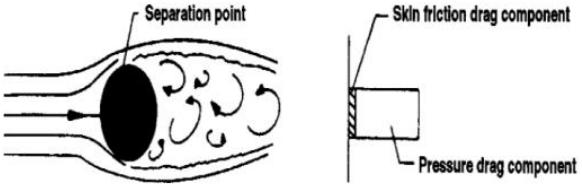

Figure 4 Flow Separation

When the separation points are on the windward side of a circular cylinder, it is easiest to see vortex shedding below the critical Reynolds number. It has been observed that the vortex street gives way to a roughly random turbulent wake above the critical Reynolds number, as the separation points further rearwards, creating a smaller wake. Periodic effects remain at Reynolds numbers considerably above the critical, as recently shown by the work of Roshko and others. This suggests that vortex shedding is a characteristic of the flow past circular cylinders over the Reynolds number range, but that the earlier research did not find the vortices because they are harder to discern.

Missile Geometry to be Investigated

The Figures 5, 6 and 7 graphics illustrate how the CATIA V20 software is used to develop the three missile geometries that will be examined for base drag. The three types under consideration are all basic hemispherical bodies with a cross sectional diameter of 50 mm and a length of 500 mm.

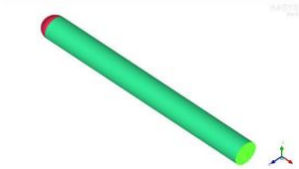

Figure 5 Flat Base

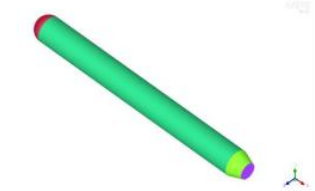

Figure 6 Boat Tail base

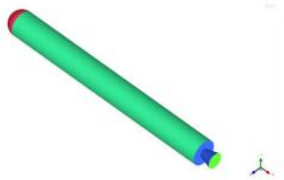

Figure 7 Nozzle Base

ICEM CFD was used to construct the grid, and the density-based solver was used.

Density Based Solver

The governing equations of continuity, momentum, and (where appropriate) energy and species transport are solved concurrently (i.e., coupled together) using the density-based solver. The process outlined in Section 4 will be employed to solve the governing equations for the additional scalars subsequently and sequentially (that is, apart from each other and from the linked set).2. A converged solution can only be reached after several iterations of the solution loop due to the non-linear (and linked) nature of the governing equations.

1. Adjust the fluid's characteristics in light of the existing solution. (If the computation is still in progress, the initialized solution will be used to update the fluid characteristics.)
2. Simultaneously solve the equations for continuity, momentum, energy, and species, where applicable.

3. When applicable, use the previously revised values of the other variables to solve equations for scalars like radiation and turbulence.
4. Use a discrete phase trajectory computation to update the source terms in the relevant continuous phase equations when interphase coupling needs to be included.
5. Verify that the set of equations is converging.

Until the convergence requirements are satisfied, these actions are repeated.

The coupled system of equations (continuity, momentum, energy, and species equations, if available) can be solved using either the coupled-explicit formulation or the coupled-implicit formulation in the density-based solution approach. The following describes the primary difference between the density-based explicit and implicit formulations. The discrete, non-linear governing equations in the density-based solution techniques are linearized to yield a system of equations for the dependent variables in each computing cell. An updated flowfield solution is then obtained by solving the resulting linear system. In terms of the dependent variable (or group of variables) of interest, the linearization process of the governing equations can be "implicit" or "explicit." The following are what we mean by implicit or explicit:

Implicit: Using a relation that contains both known and unknown values from nearby cells, the unknown value in each cell for a particular variable is calculated. Because of this, every unknown will appear in many system equations, which must all be solved at the same time in order to determine the unknown quantities.

Explicit: For a given variable, a relation that only contains values that already exist is used to compute the unknown value in each cell. As a result, every unknown will only occur in a single equation in the system, and the unknown numbers may be found by solving each equation separately for the unknown value in each cell.

Fluent is utilized for numerical solution while ANSYS ICEM CFD is used for grid creation. Using a finite volume technique, it solves the Reynolds-Averaged Navier Stokes (RANS) equations across a body-captured cartesian mesh. The boundary conditions and flow conditions are mentioned in the Table 1 and 2 respectively.

Boundary Conditions for Different Part of Geometry

Table 1: Boundary Conditions

Parts	Boundary Conditions used
Nose	Wall
Body	Wall
Boat Tail	Wall
Exhaust Dia	Wall
Farfield	Pressure Farfield

Flow Conditions

Table 2: Flow Conditions

Physical Property	Farfield	Exhaust (Pressure inlet)
Mach No.	0.15	
Initial Gauge pressure (Pa)	-	121638

Total Gauge pressure (Pa)	101325	205727
Velocity (m/s)	35	
Temperature (K)	303.15	956.33
Density (kg/m^3)	1.1638	

The Z direction points out of the paper, creating the computational domain in the X-Y plane. Left to right flow is used. D is the vehicle diameter, and the computational domain is 60D in the stream-normal direction and 100D in the stream-wise direction. To capture the geometry, each grid refinement has been made available. The purpose of providing clustering close to the geometry is to improve computing efficiency. The turbulence closure model developed by Spalart Allmaras has been used to solve RANS equations.

IV RESULTS AND DISCUSSION

CFD simulations are run for the geometry that was previously mentioned. At the missile's base, there is a noticeable shift in pressure throughout the body's length, which caused base drag. Additionally, the base's diameter is examined to determine the change in pressure, which is found to be greatest at the base's borders and lowest in the middle. The coefficient of drag was computed based on the Mach number and angle of attack that were studied, and the results are listed in the Table 3.

Table 3: CFD simulation results

Case	Velocity	Angle of attack	Cd (at base)
Flat base	20m/s	0deg	0.0792
Boat tail base	20m/s	0deg	0.0421
Nozzle base	20m/s	0deg	0.0678
Flat base	20m/s	2deg	0.0806
Boat tail base	20m/s	2deg	0.0429
Nozzle base	20m/s	2deg	0.0682
Flat base	20m/s	-2deg	0.0805
Boat tail base	20m/s	-2deg	0.0428
Nozzle base	20m/s	-2deg	0.0681
Flat base	35m/s	0deg	0.0763
Boat tail base	35m/s	0deg	0.0411
Nozzle base	35m/s	0deg	0.0678
Flat base	35m/s	2deg	0.0774
Boat tail base	35m/s	2deg	0.0412
Nozzle base	35m/s	2deg	0.0685
Flat base	35m/s	-2deg	0.0774
Boat tail base	35m/s	-2deg	0.0412
Nozzle base	35m/s	-2deg	0.0685
Flat base	50m/s	0deg	0.0759
Boat tail base	50m/s	0deg	0.0401
Nozzle base	50m/s	0deg	0.0674
Flat base	50m/s	2deg	0.0769
Boat tail base	50m/s	2deg	0.0403
Nozzle base	50m/s	2deg	0.068
Flat base	50m/s	-2deg	0.077
Boat tail base	50m/s	-2deg	0.0403
Nozzle base	50m/s	-2deg	0.0681

V CONCLUSION

By selecting the most appropriate experimental modeling and fabrication, a thorough investigation of the base drag on three missile profiles has been conducted at extremely low subsonic speeds utilizing experimental approaches. Each missile configuration's pressure distribution on its body and base was measured, and each of the three missile geometries' base pressure-related drag on the body was computed. When comparing the flat base configuration and nozzle configuration to the boat tail design, which only considers drag at the boat tail shroud and the nozzle flare section, the predicted values of the coefficient of base drag (C_{db}) were found to be greater. However, if we just take into account the base, the base drag coefficient (Cdb) for the boat tail and flat base design is raised, approaching that of the nozzle base by a tiny amount. But compared to the baseline arrangement, where the drag increases significantly with increasing velocity and angle of attack, the Cdb for the nozzle configuration was found to be lower. Comparing the results for the three scenarios, it was concluded that the base's boat tailing with the predicted drag at the boat tail's shroud would be a useful design strategy for the body that reduces the projectile's drag. This decrease in drag may be used to explain the missile's increased range, which makes it extremely advantageous for military uses.

VI REFERENCES

[1] Sethunathan, P., Sugendran, R. N., & Anbarasan, T. (2015). Aerodynamic configuration design of missile. *International Journal of Engineering Research & Technology*, *4*(3), 72-75.

[2] Karpov, B. G. (1965). *The Effect of Various Boattail Shapes on Base Pressure and Other Aerodynamic Characteristics of a 7-Caliber Long Body of Revolution at M=1.70*. Ballistic Research Laboratories Report no. 1295.

[3] Wee, H. C. (2011). *Aerodynamic Analysis of a Canard Missile Configuration using ANSYS-CFX*. Naval Postgraduate School.

[4] Lee, K. S., & Hong, S. K. (2007). CFD applications and validations in aerodynamic design and analysis for missiles. *International Symposium on Integrating CFD and Experiments in Aerodynamics*.

[5] Brebner, G. G. (1979). *A Brief Review of Air Flight Weapons*. Advisory Group for Aerospace Research and Development.

[6] Mitchell, R., Webb, M., Roetzel, J., Lu, F., & Dutton, J. (2008). A study of the base pressure distribution of a slender body of square cross-section. *AIAA Aerospace Sciences Meeting and Exhibit*.

[7] Hitchcock, H. P. (1951). *On Estimating the Drag Coefficient of Missiles*. Ballistic Research Laboratories Memorandum report no. 545.

[8] Moore, F., Hymer, T., & Wilcox, F. J. (1992). *Improved Empirical Model for Base Drag Prediction on Missile Configurations based on New Wind Tunnel Data*. Naval Surface Warfare Center.

[9] Menezes, V., Takayama, K., Sun, M., Gopalan, J., & Reddy, K. P. J. (2012). Drag reduction by controlled base flow separation. *Journal of Aircraft*, *43*(5).